Truncation-dependent math xmlns="http://www.w3.org/1998/Math/MathML">mi mathvariant="script">PT/mi>/math> phase transition for the edge states of a two-dimensional non-Hermitian system

Dali Cheng, Bo Peng, Meng Xiao, Xianfeng Chen, Luqi Yuan, and Shanhui Fan

Phys. Rev. B **105**, L201105 — Published 6 May 2022

DOI: 10.1103/PhysRevB.105.L201105

Truncation-dependent *PT* phase transition for the edge states of a two-dimensional non-Hermitian system

Dali Cheng,[1,2] Bo Peng,[2] Meng Xiao,[3] Xianfeng Chen,[2,4,5,6] Luqi Yuan,[2,*] and Shanhui Fan[1]

[1]*Ginzton Laboratory and Department of Electrical Engineering, Stanford University, Stanford, California 94305, USA*

[2]*State Key Laboratory of Advanced Optical Communication Systems and Networks, School of Physics and Astronomy, Shanghai Jiao Tong University, Shanghai 200240, China*

[3]*School of Physics and Technology, Center for Nanoscience and Nanotechnology, and Key Laboratory of Artificial Micro- and Nano-structures of Ministry of Education, Wuhan University, Wuhan 430072, China*

[4]*Shanghai Research Center for Quantum Sciences, Shanghai 201315, China*

[5]*Jinan Institute of Quantum Technology, Jinan 250101, China*

[6]*Collaborative Innovation Center of Light Manipulation and Applications, Shandong Normal University, Jinan 250358, China*

[*]yuanluqi@sjtu.edu.cn

Abstract

We consider a bulk system supporting parity and time reversal (*PT*) symmetry, and investigate how the *PT* phase transition of edge states is influenced by different truncations of the system. As an example, we study a two-dimensional *PT*-symmetric Su–Schrieffer–Heeger lattice with non-Hermitian onsite potentials. We find that when the truncation preserves certain symmetries of the bulk lattice, the edge states can remain in the *PT*-unbroken phase when the non-Hermitian onsite potentials are below a non-zero critical value. On the other hand, when the truncation removes such symmetries, edge states with complex eigen-energies are observed for infinitesimal non-Hermitian onsite potentials. We develop an analytic theory to account for such behaviors. Our results are important in the manipulation of the gain and loss behaviors of edge states in non-Hermitian systems, with potential applications in the study of topological lasers, quantum sensors and unidirectional invisibility.

A finite-sized physical system may support edge states localized at the boundaries of its bulk. These states play an important role in determining the physical properties of finite-sized physical systems [1-3]. In the field of photonics, edge states can be found in a wide variety of systems including photonic crystals, metamaterials, and plasmonic structures [4-7]. These states find applications for the guiding of light in information and sensing applications [8,9].

Recently, physical systems with parity and time reversal (*PT*) symmetries have generated significant interests [10-14]. In particular, bulk periodic systems with PT symmetries have been extensively studied [15-23], and it was noted that these systems can feature a PT phase transition between a PT-unbroken phase with a real eigen-spectrum, and a PT-broken phase with a complex eigen-spectrum [15,16,18-20,23,24]. Since these systems, when truncated, may support edge states, it should be of interest to explore the possible PT phase transitions for the edge states, and to contrast the phase-transition behaviors between the bulk and the edge states. Thus, there have been many results on edge (and interface) states in one-dimensional (1D) PT-symmetric systems [25-43]. Edge states in 2D PT-symmetric systems have also been explored, and both PT-broken and PT-unbroken phases have been observed in different systems [44-49]. In two dimensions, different truncations of the same periodic system can lead to different boundary geometries. However, there has not been an investigation of how the PT phase transition behaviors of edge states in 2D systems are influenced by different truncations.

In this letter, we show that different PT phase transition behaviors of edge states can be achieved by varying the truncation of a 2D periodic system. As an illustration, we study a 2D PT-symmetric Su–Schrieffer–Heeger (SSH) lattice with non-Hermitian onsite potentials, and we truncate the lattice in different orientations. These truncations usually lead to localized edge states. We find that, when the truncation features certain symmetries, the associated edge states can be in the PT-unbroken phase when the strength of the non-Hermitian onsite potential is small. On the other hand, for a truncation without such symmetries, the edge states always have complex eigen-energies for any infinitesimal strength of the non-Hermitian onsite potential. Our result provides an understanding of the interplay between boundary geometries and eigenstate properties in non-Hermitian systems, and may be useful in the design and engineering of edge states in various photonic applications such as the design of topological lasers [50-52].

We start our theoretical analysis by considering a non-Hermitian 2D SSH lattice, as shown in Fig. 1(a). The lattice is periodic along both x and y directions, and a primitive cell contains four inequivalent lattice sites, which are indicated with coordinates (xa, ya), $((x+1/2)a, ya)$, $(xa, (y+1/2)a)$, and $((x+1/2)a, (y+1/2)a)$, respectively ($x, y \in \mathbb{Z}$, and a is the lattice constant). The intra-cell and inter-cell coupling strengths are denoted by g_1 and g_2, respectively. Both g_1 and g_2 are assumed to be real. Gain and loss with the same magnitude $U \geq 0$ in their strength are introduced on each (xa, ya) sites and $((x+1/2)a, (y+1/2)a)$ sites, respectively. The Hamiltonian of such system is $H = H_0 + V$, where

$$H_0=\sum_{x,y}\left[g_1\left(b^\dagger_{x+1/2,y}+b^\dagger_{x,y+1/2}\right)\left(b_{x,y}+b_{x+1/2,y+1/2}\right)+g_2\left(b^\dagger_{x+1/2,y+1}+b^\dagger_{x+1,y+1/2}\right)\left(b_{x+1,y+1}+b_{x+1/2,y+1/2}\right)+\text{h.c.}\right],$$
$$V=iU\sum_{x,y}\left(b^\dagger_{x,y}b_{x,y}-b^\dagger_{x+1/2,y+1/2}b_{x+1/2,y+1/2}\right), \tag{1}$$

where b ($b^\dagger$) is the bosonic annihilation (creation) operator at the corresponding lattice site. Here H_0 (V) gives the Hermitian (anti-Hermitian) part of the Hamiltonian, i.e. $H_0 = H_0^\dagger$ and $V = -V^\dagger$. The full Hamiltonian is PT-symmetric, i.e. $(PT)^{-1}H(PT) = H$, where the parity operator P is defined as the inversion operation around the point $((x+1/4)a, (y+1/4)a)$, and T is the standard time-reversal operation. The corresponding band structure of this Hamiltonian is

$$E\left(k_x,k_y\right)=\pm\sqrt{\left|g_1+g_2\exp\left(ik_xa\right)\right|^2-\frac{U^2}{4}}\pm\sqrt{\left|g_1+g_2\exp\left(ik_ya\right)\right|^2-\frac{U^2}{4}}, \tag{2}$$

where k_x (k_y) is the wavevector along the x (y) axis. The band structure for $U = 0$, $g_1 = g$, $g_2 = 5g$ is plotted in Fig. 2(a). Four bands are observed because each primitive cell contains four sites. The two middle bands are degenerate at zero energy when $k_x = \pm k_y$, and they are gapped from the other two bands. As seen from Eq. (2), there is a phase transition occurring at a critical value of $U_C^{\text{bulk}} = 2|g_1 - g_2|$. When $U \le 2|g_1 - g_2|$, the energy spectrum is real throughout the entire reciprocal space. When $U > 2|g_1 - g_2|$, the energy spectrum becomes complex for at least some of the wavevectors, and the system undergoes a phase transition entering the PT-broken phase.

A one-dimensional SSH lattice is well known as one of the simplest topological models [53]. With certain choices of parameters the periodic lattice exhibits a non-zero Zak phase [54], which guarantees localized edge states when the lattice is truncated. For the 2D case as we consider here, there is also a non-zero Zak phase along any direction inside the Brillouin zone when $g_2 > g_1$. Here, the vectorized Zak phase for the 2D Hermitian SSH model is defined as [55,56]:

$$\boldsymbol{\theta} = -\frac{1}{2\pi}\int_{\text{BZ}} \mathrm{d}^2\boldsymbol{k}\sum_n i\langle u_n(\boldsymbol{k})|\nabla_{\boldsymbol{k}}|u_n(\boldsymbol{k})\rangle, \tag{3}$$

where $|u_n(\mathbf{k})\rangle$ is the periodic part of the Bloch wavefunction of the n-th band in the reciprocal space [55]. The summation is taken over all bands. The j-th component of the vectorized Zak phase is

$$\theta_j = 2\int_{-\pi/a}^{\pi/a}\mathrm{d}k_j\frac{\partial}{\partial k_j}\arg\left(g_1+g_2\mathrm{e}^{ik_ja}\right),\ j=x,y, \tag{4}$$

The quantity $f\left(k_j\right) = g_1 + g_2\mathrm{e}^{ik_ja}$ lies in a complex plane. For $g_2 < g_1$, the origin of the complex plane is outside the circle defined by $f\left(k_j\right)$ as k_j varies across the Brillouin Zone from $-\pi/a$ to π/a, and θ_j is zero, while for $g_2 > g_1$, the origin is inside the circle, giving rise to a non-zero θ_j. Thus, there are also localized edge states with a topological origin. In particular, for the lattice that we consider, when the Zak phase is non-zero, all the edge states inside the gap in our model have a topological origin. Moreover, there is an additional richness in the edge state behaviors since we can choose different orientations for the truncation of the lattice. In Figs. 1(b)–1(d), we provide an illustration of three truncation configurations as examples. The truncations are set to be (10) surface (Fig. 1(b), parallel to the $\hat{\mathbf{x}}$ direction), (11) surface (Fig. 1(c), parallel to the $\hat{\mathbf{x}}+\hat{\mathbf{y}}$ direction) and (21) surface (Fig. 1(d), parallel to the $2\hat{\mathbf{x}} + \hat{\mathbf{y}}$ direction), respectively. In all of the three truncations, the four-site primitive cell structure is preserved on the boundaries of lattices.

Throughout the paper we present theoretical analysis for semi-infinite structures with a single truncation. In the numerical analysis, however, we present results on large finite stripes, which will be shown in Fig. 2. The Hamiltonian that we analyze in this paper does not have a non-trivial point gap topology, and hence does not exhibit non-Hermitian skin effects [57-60]. Therefore, the results from a large finite stripe are rather similar to those from the corresponding semi-infinite system. In the finite stripe we have pairs of edge states residing on either end of the stripe, and the spectrum of each member of the pair is essentially identical to that of the edge state in the semi-infinite system.

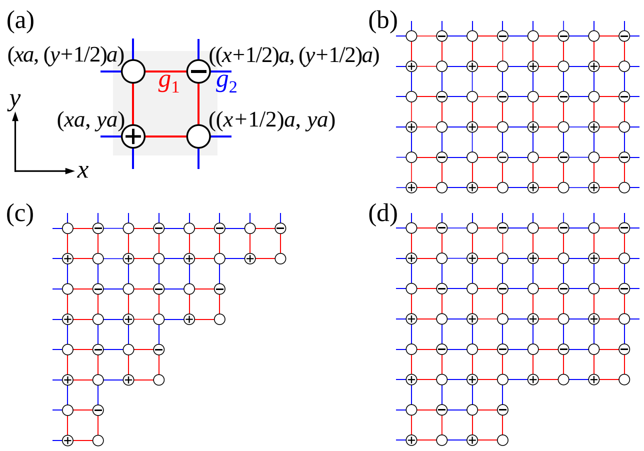

Fig. 1 Two-dimensional SSH lattices and different truncation configurations. (a) A primitive cell of the 2D SSH lattice, as shaded in grey. Intra-cell (inter-cell) couplings are shown in red (blue), and gains (losses) are shown by plus (minus) sign. (b)–(d) 2D SSH lattices with the (b) (10), (c) (11), (d) (21) truncation configurations.

The truncated SSH lattices in Figs. 1(b)–1(d) has translational symmetry only in one direction, and the associated projected band structures are shown in Figs. 2(b)–2(h), in the topologically nontrivial phase ($g_1 = g$, $g_2 = 5g$). Projected band structures of Hermitian systems ($U = 0$) are plotted in Figs. 2(b), 2(e) and 2(g) with different truncation configurations. Here k_p is the wavevector parallel to the truncation. In these projected band structures, the bulk states can be obtained by projecting the 2D band structure as shown in Fig. 2(a) onto appropriate lines in the reciprocal space and by performing band folding if necessary. In such projections $k_p = k_x$ for the (10) truncation, $k_p = (k_x + k_y)/\sqrt{2}$ for the (11) truncation, and $k_p = (2k_x + k_y)/\sqrt{5}$ for (21) truncation. These bulk states are separated by band gaps. Moreover, isolated edge states are observed inside the band gaps. Both the (10) and (11) truncations have two edge states, while the (21) truncation features four, thus the number of edge states is dependent on the lattice truncation [61].

Next, we move onto the non-Hermitian case ($U > 0$). Above we have shown that the bulk band structure undergoes a *PT* phase transition at $U_C^{\text{bulk}} = 2|g_1 - g_2|$. Here we show that the edge states also undergo a phase transition, but the transition behaviors are distinctly different from the bulk and dependent critically on the orientations of the truncations. Figs. 2(f) and 2(h) give the projected band structures of non-Hermitian lattices for the (10) and (21) truncations, respectively, with $U = 10^{-3}g$. One sees that the energies of edge states exhibit non-zero imaginary parts across the entire *k*-space. The eigen-energies of the bulk states, on the other hand, remain real-valued. In other words, for the edge states associated with the (10) and (21) truncations, the phase transition occurs at an infinitesimal strength of non-Hermiticity, and the critical values are $U_C^{(10)} = U_C^{(21)} = 0$. This result of the (10) truncation is consistent with previous literature [48].

The projected band structures of the (11) truncation are shown in Figs. 2(c) and 2(d) with different values of the non-Hermiticity strength *U*. In contrast to the (10) and (21) truncations, here the eigen-energies of all edge states are still real when $U = 3g$. As the non-Hermiticity strength is further increased and reaches $U_C^{(11)} \approx 5.65g$, the edge states merge with the highest-energy bulk states in the middle bands near $|k_p| = \pm\pi/\sqrt{2}a$, and a phase transition occurs. In Fig. 2(d), the projected band structure when $U = 5.7g$ is plotted, the eigen-energies of the edge states become complex in the wavevector range of $|k_p| < 0.81\pi/\sqrt{2}a$, and exceptional points are found at $|k_p| \approx 0.81\pi/\sqrt{2}a$. This phase transition with a non-zero critical value is unique to the (11) truncation; for this system any other (*mn*) boundary truncation ($m \neq n, m, n \in \mathbb{Z}$) has $U_C = 0$.

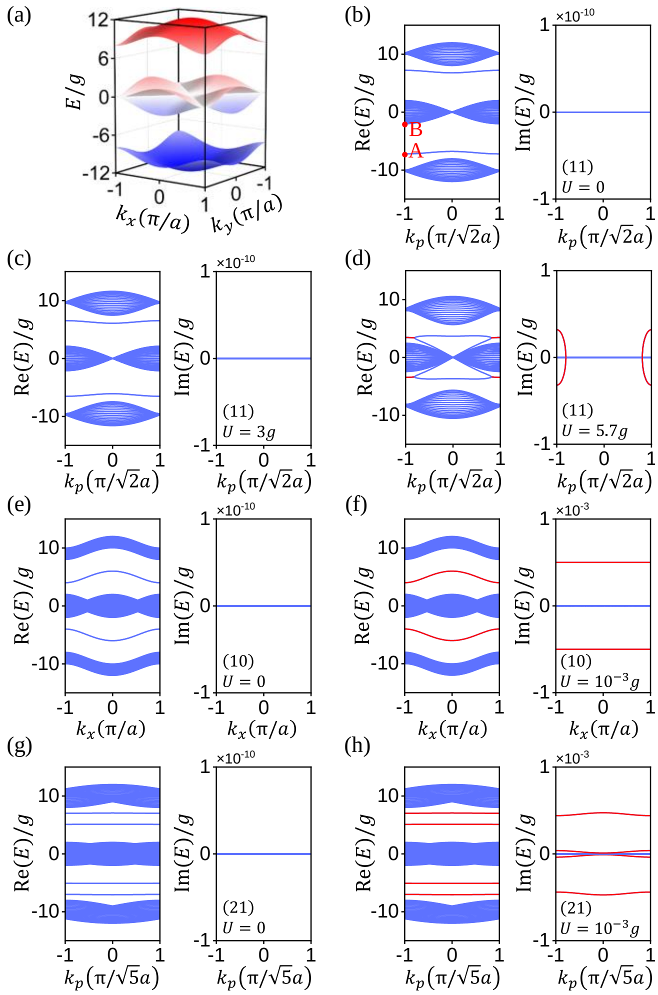

Fig. 2 Band structures of periodic and truncated 2D SSH lattice when $g_1 = g$, $g_2 = 5g$. (a) Band structure of periodic (bulk) 2D SSH lattice. (b)–(d) Projected band structures of a 2D SSH lattice with a (11) truncation when (b) $U = 0$, (c) $U = 3g$, (d) $U = 5.7g$. (e)–(f) Projected band structures of a 2D SSH lattice with a (10) truncation when (e) $U = 0$, (f) $U = 10^{-3}g$. (g)–(h) Projected band structures of a 2D SSH lattice with a (21) truncation when (g) $U = 0$, (h) $U = 10^{-3}g$. In (b)–(h), $N = 21$ layers of primitive cells along the y direction are used for numerical calculations, instead of the semi-infinite lattices in Figs. 1(b)–1(d). Eigen-energies with non-zero imaginary parts are in red.

In order to understand the different behaviors of the edge states for different truncations, below we provide theoretical arguments from the perspective of symmetry analysis. The semi-infinite non-Hermitian systems with (10) and (21) truncations are not PT-symmetric for any spatial symmetry operation P. Thus generically the energy eigenvalues become complex with infinitesimal non-Hermiticity strength. On the other hand, for the system with the (11) truncation, although the PT symmetry associated with the inversion operation in the 2D bulk SSH lattice disappears, the system has an RT symmetry, where R is the mirror symmetry associated with the reflection operation against the $\hat{\mathbf{x}} - \hat{\mathbf{y}}$ direction.

The behavior of the edge states for the (11) truncation is directly related to the symmetry property of the lattice. In the lattice with the (11) truncation, when $U = 0$, we use $|\phi_0\rangle$ and $|\phi_1\rangle$ to respectively denote the edge and the corresponding bulk states involved in the phase transition at a specific k_p point. Here both $|\phi_0\rangle$ and $|\phi_1\rangle$ are eigenstates of the Hermitian part of the Hamiltonian as denoted by $H_0^{(11)}$, and the chosen bulk state $|\phi_1\rangle$ is the state exactly at the edge of the gap. In Fig. 3, we plot the distributions of $|\phi_i\rangle$ at $k_p = \pm\pi/\sqrt{2}a$, where the edge state $|\phi_0\rangle$ has odd RT symmetry, and the bulk state $|\phi_1\rangle$ has even RT symmetry. Below, to simplify the notation, we suppress the superscripts (11) with the understanding that the Hamiltonian refers to that of truncated lattice rather than the bulk Hamiltonian in Eq. (1).

As a simple model, we describe the phase transition process in the Hilbert space spanned by $|\phi_0\rangle$ and $|\phi_1\rangle$, with the matrix elements of the Hamiltonian in this Hilbert space calculated as:

$$H_{ij} = \langle\phi_i|H_0 + V|\phi_j\rangle = E_j\delta_{ij} + \langle\phi_i|V|\phi_j\rangle, i, j = 0, 1. \tag{5}$$

In Eq. (5), E_i is the eigen-energy for the state $|\phi_i\rangle$. The last term $V_{ij} = \langle\phi_i|V|\phi_j\rangle$ arises from the gain or loss added to the lattice sites. By noticing that $V^\dagger = -V$, one can obtain

$$\langle\phi_i|V|\phi_j\rangle^* = \langle\phi_j|V^\dagger|\phi_i\rangle = -\langle\phi_j|V|\phi_i\rangle. \tag{6}$$

Therefore, we have $V_{ii}^* = -V_{ii}$, so V_{ii} is purely imaginary. Also, the off-diagonal elements of the coupling matrix can be written as

$$V_{01} = (\gamma + i\kappa)U, V_{10} = (-\gamma + i\kappa)U,\ \gamma, \kappa \in \mathbb{R}, \tag{7}$$

where γ and κ are independent of the strength of the non-Hermiticity U. Since the lattice with the (11) truncation has the RT symmetry, we have:

$$(RT)^{-1}H_0(RT) = H_0, \tag{8}$$

$$(RT)^{-1}V(RT) = V. \tag{9}$$

Because of Eq. (8), the non-degenerate eigenstates of H_0 satisfy

$$RT|\phi_i\rangle = r_i|\phi_i\rangle,\ r_i = \pm1,\ i = 0,1. \tag{10}$$

By combining Eqs. (9) and (10), we have

$$r_j\langle\phi_i|V|\phi_j\rangle = \langle\phi_i|VRT|\phi_j\rangle = \langle\phi_i|RTV|\phi_j\rangle = \langle RT\phi_i|V|\phi_j\rangle^* = r_i\langle\phi_i|V|\phi_j\rangle^*, \tag{11}$$

which indicates that V_{ii} is real. V_{ii} is both real and purely imaginary, so one concludes

$$V_{ii} = 0. \tag{12}$$

Also, since for our system $r_0 = -r_1$, we have $V_{10} = -V_{10}^*$. Therefore, combining with Eq. (7) we have

$$V_{01} = V_{10} = i\kappa U. \tag{13}$$

Therefore, from Eqs. (5), (12) and (13), we obtain a matrix form of the Hamiltonian:

$$H = \begin{bmatrix} E_0 & i\kappa U \\ i\kappa U & E_1 \end{bmatrix}, \tag{14}$$

and its eigenvalues are

$$E_\pm = \frac{E_0+E_1}{2} \pm \frac{\sqrt{(E_0-E_1)^2-4\kappa^2U^2}}{2}. \tag{15}$$

From Eq. (15), one finds that, when $0 < U \leq U_C = \min_{k_p} |E_0 - E_1|/(2\kappa)$, both the edge state and bulk state remain real-valued energies. Moreover, when the dimerization ratio g_2/g_1 becomes larger, $|E_0 - E_1|$ increases, and therefore the critical value of the *PT* phase transition U_C increases.

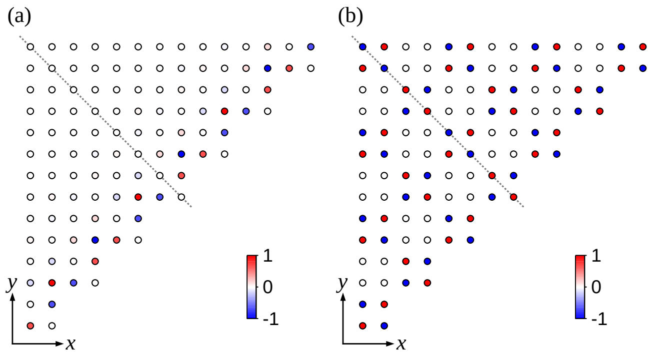

Fig. 3 Eigenstate distributions with the (11) truncation with *RT* symmetry. (a) The edge state at Point A in Fig. 2(b). The state is anti-symmetric against to the grey dashed line. (b) The bulk state at Point B in Fig. 2(b). The state is symmetric against the grey dashed line. The eigenstate magnitudes on lattice sites are normalized with respect to the maximum value in the whole lattice.

Our results above point to a connection between a non-zero critical value of phase transition in Eq. (15), and the existence of *RT* symmetry for both H_0 and V (Eqs. (8) and (9)). In our system, lattices with truncations other than (11) do not exhibit *RT* symmetry and hence the phase transition occur at infinitesmal strength of the non-Hermiticity. Such an approach based on symmetry analysis could be applied to other non-Hermitian 2D systems as well. For example, we can numerically verify the *PT* phase transition of the strained graphene lattice with onsite gains and losses as studied in [47]. With the bearded or zigzag truncations, the honeycomb lattice does not feature any *RT* symmetry, and the lattice is in the *PT*-broken phase for infinitesimal strength of the non-Hermiticity when edge states are present. The lattice with the armchair truncation has an additional *RT* symmetry and hence a non-zero critical value U_C for the phase transition. For the armchair truncation for this system there is no edge state, thus the phase transition occurs through the coalescence of two bulk states. The edge states considered here have topological origins, but their *PT* phase transition behaviors are not directly and causally related to the topological properties, since the topological properties are determined by the bulk Hamiltonian, whereas the properties of the *PT* phase transition are affected by the symmetries of the truncations. The importance of symmetry consideration in *PT* phase transition has been noted in a number of studies on some one-dimensional [30] and two-dimensional [46] lattices, or more generally on the wave equations [62] and topological many-body systems [63] with degeneracy. Our work differs in that we use the symmetry analysis to study the dependence of the phase transition of the edge states on the lattice truncations.

In summary, we investigate the truncation dependence of the *PT* phase transition of edge states in a 2D physical system where the bulk periodic system has *PT* symmetry. Our results show that, with specific truncation configurations (such as the (11) truncation), the truncated system preserves certain symmetry properties of the bulk periodic system, and consequently the critical value of the *PT* phase transition is non-zero for the edge states. The edge states remain in the *PT*-unbroken phase when the non-Hermiticity is within the critical value. For other configurations where the truncation breaks the symmetry of the bulk, the eigen-energies exhibit non-zero imaginary parts and edge states experience gain and loss for infinitesimal non-Hermiticity. Our theoretical study here is applicable to a variety of experimental platforms that have been used to construct two-dimensional periodic lattice, such as photonic waveguide arrays, resonator arrays and cavity arrays [64-68], cold bosonic atoms in optical lattices [69,70], superconducting circuits [71-73], and artificial lattices with synthetic dimensions [74-78]. The results and arguments presented in this letter are expected to provide insights into research that requires the engineering of the critical values of the *PT* phase transition of edge states in multi-dimensional physical systems, for example, in the studies of sensing, topological lasing and unidirectional invisibility near a *PT* phase transition point [13,14,79,80].

Acknowledgements

The authors are grateful for helpful discussions with Prof. Zhong Wang. The research is supported by National Natural Science Foundation of China (12122407, 11974245), National Key R&D Program of China (2017YFA0303701), Shanghai Municipal Science and Technology Major Project (2019SHZDZX01), and Natural Science Foundation of Shanghai (19ZR1475700). L. Y. acknowledges support from the Program for Professor of Special Appointment (Eastern Scholar) at Shanghai Institutions of Higher Learning. X. C. acknowledges support from Shandong Quancheng Scholarship (00242019024). S. F. acknowledges the support of a Vannevar Bush Faculty Fellowship from the U. S. Department of Defense (Grant No. N00014-17-1-3030), and a Simons Investigator in Physics grant from the Simons Foundation (Award No. 827065).

References

[1] W. Shockley, *On the surface states associated with a periodic potential*, Physical Review **56**, 317 (1939).

[2] A. H. Castro Neto, F. Guinea, N. M. R. Peres, K. S. Novoselov, and A. K. Geim, *The electronic properties of graphene*, Reviews of Modern Physics **81**, 109 (2009).

[3] M. Z. Hasan and C. L. Kane, *Colloquium: Topological insulators*, Reviews of Modern Physics **82**, 3045 (2010).

[4] R. D. Meade, K. D. Brommer, A. M. Rappe, and J. D. Joannopoulos, *Electromagnetic Bloch waves at the surface of a photonic crystal*, Physical Review B **44**, 10961 (1991).

[5] W. L. Barnes, A. Dereux, and T. W. Ebbesen, *Surface plasmon subwavelength optics*, Nature **424**, 824 (2003).

[6] L. Lu, J. D. Joannopoulos, and M. Soljačić, *Topological photonics*, Nature Photonics **8**, 821 (2014).

[7] T. Ozawa, H. M. Price, A. Amo, N. Goldman, M. Hafezi, L. Lu, M. C. Rechtsman, D. Schuster, J. Simon, O. Zilberberg *et al.*, *Topological photonics*, Reviews of Modern Physics **91**, 015006 (2019).

[8] F. Villa, L. E. Regalado, F. Ramos-Mendieta, J. Gaspar-Armenta, and T. Lopez-Ríos, *Photonic crystal sensor based on surface waves for thin-film characterization*, Opt. Lett. **27**, 646 (2002).

[9] S. Barik, A. Karasahin, C. Flower, T. Cai, H. Miyake, W. DeGottardi, M. Hafezi, and E. Waks, *A topological quantum optics interface*, Science **359**, 666 (2018).

[10] C. E. Rüter, K. G. Makris, R. El-Ganainy, D. N. Christodoulides, M. Segev, and D. Kip, *Observation of parity–time symmetry in optics*, Nature Physics **6**, 192 (2010).

[11] A. A. Zyablovsky, A. P. Vinogradov, A. A. Pukhov, A. V. Dorofeenko, and A. A. Lisyansky, *PT-symmetry in optics*, Physics-Uspekhi **57**, 1063 (2014).

[12] L. Feng, Z. J. Wong, R.-M. Ma, Y. Wang, and X. Zhang, *Single-mode laser by parity-time symmetry breaking*, Science **346**, 972 (2014).

[13] L. Feng, R. El-Ganainy, and L. Ge, *Non-Hermitian photonics based on parity–time symmetry*, Nature Photonics **11**, 752 (2017).

[14] Ş. K. Özdemir, S. Rotter, F. Nori, and L. Yang, *Parity–time symmetry and exceptional points in photonics*, Nature Materials **18**, 783 (2019).

[15] Z. H. Musslimani, K. G. Makris, R. El-Ganainy, and D. N. Christodoulides, *Optical solitons in PT periodic potentials*, Physical Review Letters **100**, 030402 (2008).

[16] K. G. Makris, R. El-Ganainy, D. N. Christodoulides, and Z. H. Musslimani, *Beam dynamics in PT symmetric optical lattices*, Physical Review Letters **100**, 103904 (2008).

[17] S. Longhi, *Bloch oscillations in complex crystals with PT symmetry*, Physical Review Letters **103**, 123601 (2009).

[18] Z. Lin, H. Ramezani, T. Eichelkraut, T. Kottos, H. Cao, and D. N. Christodoulides, *Unidirectional invisibility induced by PT-symmetric periodic structures*, Physical Review Letters **106**, 213901 (2011).

[19] A. Regensburger, C. Bersch, M.-A. Miri, G. Onishchukov, D. N. Christodoulides, and U. Peschel, *Parity–time synthetic photonic lattices*, Nature **488**, 167 (2012).

[20] M. Wimmer, A. Regensburger, M.-A. Miri, C. Bersch, D. N. Christodoulides, and U. Peschel, *Observation of optical solitons in PT-symmetric lattices*, Nature Communications **6**, 7782 (2015).

[21] M. Wimmer, M.-A. Miri, D. Christodoulides, and U. Peschel, *Observation of Bloch oscillations in complex PT-symmetric photonic lattices*, Scientific Reports **5**, 17760 (2015).

[22] Y.-L. Xu, W. S. Fegadolli, L. Gan, M.-H. Lu, X.-P. Liu, Z.-Y. Li, A. Scherer, and Y.-F. Chen, *Experimental realization of Bloch oscillations in a parity-time synthetic silicon photonic lattice*, Nature Communications **7**, 11319 (2016).

[23] Z. Zhang, Y. Zhang, J. Sheng, L. Yang, M.-A. Miri, D. N. Christodoulides, B. He, Y. Zhang, and M. Xiao, *Observation of parity-time symmetry in optically induced atomic lattices*, Physical Review Letters **117**, 123601 (2016).

[24] A. Cerjan, A. Raman, and S. Fan, *Exceptional contours and band structure design in parity-time symmetric photonic crystals*, Physical Review Letters **116**, 203902 (2016).

[25] B. Zhu, R. Lü, and S. Chen, *PT symmetry in the non-Hermitian Su-Schrieffer-Heeger model with complex boundary potentials*, Physical Review A **89**, 062102 (2014).

[26] C. Poli, M. Bellec, U. Kuhl, F. Mortessagne, and H. Schomerus, *Selective enhancement of topologically induced interface states in a dielectric resonator chain*, Nature Communications **6**, 6710 (2015).

[27] C. Yuce, *Topological phase in a non-Hermitian PT symmetric system*, Physics Letters A **379**, 1213 (2015).

[28] X. Wang, T. Liu, Y. Xiong, and P. Tong, *Spontaneous PT-symmetry breaking in non-Hermitian Kitaev and extended Kitaev models*, Physical Review A **92**, 012116 (2015).

[29] H. Zhao, S. Longhi, and L. Feng, *Robust light state by quantum phase transition in non-Hermitian optical materials*, Scientific Reports **5**, 17022 (2015).

[30] A. K. Harter, T. E. Lee, and Y. N. Joglekar, *PT-breaking threshold in spatially asymmetric Aubry-André and Harper models: Hidden symmetry and topological states*, Physical Review A **93**, 062101 (2016).

[31] S. Weimann, M. Kremer, Y. Plotnik, Y. Lumer, S. Nolte, K. G. Makris, M. Segev, M. C. Rechtsman, and A. Szameit, *Topologically protected bound states in photonic parity–time-symmetric crystals*, Nature Materials **16**, 433 (2017).

[32] M. Klett, H. Cartarius, D. Dast, J. Main, and G. Wunner, *Relation between PT-symmetry breaking and topologically nontrivial phases in the Su-Schrieffer-Heeger and Kitaev models*, Physical Review A **95**, 053626 (2017).

[33] L. Jin, P. Wang, and Z. Song, *Su-Schrieffer-Heeger chain with one pair of PT-symmetric defects*, Scientific Reports **7**, 5903 (2017).

[34] L. Xiao, X. Zhan, Z. H. Bian, K. K. Wang, X. Zhang, X. P. Wang, J. Li, K. Mochizuki, D. Kim, N. Kawakami *et al.*, *Observation of topological edge states in parity–time-symmetric quantum walks*, Nature Physics **13**, 1117 (2017).

[35] L. Jin, *Topological phases and edge states in a non-Hermitian trimerized optical lattice*, Physical Review A **96**, 032103 (2017).

[36] S. Lieu, *Topological phases in the non-Hermitian Su-Schrieffer-Heeger model*, Physical Review B **97**, 045106 (2018).

[37] C. Yuce, *Edge states at the interface of non-Hermitian systems*, Physical Review A **97**, 042118 (2018).

[38] C. Yuce, *Stable topological edge states in a non-Hermitian four-band model*, Physical Review A **98**, 012111 (2018).

[39] Z.-X. Kong, Y.-F. Zhang, H.-X. Hao, and W.-J. Gong, *Energy spectra of coupled Su-Schrieffer-Heeger chains with PT-symmetric imaginary boundary potentials*, Physica Scripta **95**, 115801 (2020).

[40] S. Xia, D. Kaltsas, D. Song, I. Komis, J. Xu, A. Szameit, H. Buljan, K. G. Makris, and Z. Chen, *Nonlinear tuning of PT symmetry and non-Hermitian topological states*, Science **372**, 72 (2021).

[41] A. Stegmaier, S. Imhof, T. Helbig, T. Hofmann, C. H. Lee, M. Kremer, A. Fritzsche, T. Feichtner, S. Klembt, S. Höfling *et al.*, *Topological defect engineering and PT symmetry in non-Hermitian electrical circuits*, Physical Review Letters **126**, 215302 (2021).

[42] S. Longhi, *PT-symmetric optical superlattices*, Journal of Physics A: Mathematical and Theoretical **47**, 165302 (2014).

[43] M. Pan, H. Zhao, P. Miao, S. Longhi, and L. Feng, *Photonic zero mode in a non-Hermitian photonic lattice*, Nature Communications **9**, 1308 (2018).

[44] K. Esaki, M. Sato, K. Hasebe, and M. Kohmoto, *Edge states and topological phases in non-Hermitian systems*, Physical Review B **84**, 205128 (2011).

[45] Z. Oztas and C. Yuce, *Spontaneously broken particle-hole symmetry in photonic graphene with gain and loss*, Physical Review A **98**, 042104 (2018).

[46] X. Ni, D. Smirnova, A. Poddubny, D. Leykam, Y. Chong, and A. B. Khanikaev, *PT phase transitions of edge states at PT symmetric interfaces in non-Hermitian topological insulators*, Physical Review B **98**, 165129 (2018).

[47] M. Kremer, T. Biesenthal, L. J. Maczewsky, M. Heinrich, R. Thomale, and A. Szameit, *Demonstration of a two-dimensional PT-symmetric crystal*, Nature Communications **10**, 435 (2019).

[48] C. Yuce and H. Ramezani, *Topological states in a non-Hermitian two-dimensional Su-Schrieffer-Heeger model*, Physical Review A **100**, 032102 (2019).

[49] S. Fan, Y. Xing, L. Qi, H.-F. Wang, and S. Zhang, *Defect-position-dependent PT-symmetry breaking in coupled Su–Schrieffer–Heeger chains*, Laser Physics Letters **16**, 125203 (2019).

[50] M. Parto, S. Wittek, H. Hodaei, G. Harari, M. A. Bandres, J. Ren, M. C. Rechtsman, M. Segev, D. N. Christodoulides, and M. Khajavikhan, *Edge-mode lasing in 1D topological active arrays*, Physical Review Letters **120**, 113901 (2018).

[51] A. Y. Song, X.-Q. Sun, A. Dutt, M. Minkov, C. Wojcik, H. Wang, I. A. D. Williamson, M. Orenstein, and S. Fan, *PT-symmetric topological edge-gain effect*, Physical Review Letters **125**, 033603 (2020).

[52] Z. Chen and M. Segev, *Highlighting photonics: looking into the next decade*, eLight **1**, 2 (2021).

[53] W. P. Su, J. R. Schrieffer, and A. J. Heeger, *Solitons in Polyacetylene*, Physical Review Letters **42**, 1698 (1979).

[54] J. Zak, *Berry's phase for energy bands in solids*, Physical Review Letters **62**, 2747 (1989).

[55] D. Obana, F. Liu, and K. Wakabayashi, *Topological edge states in the Su-Schrieffer-Heeger model*, Physical Review B **100**, 075437 (2019).

[56] M. Kim and J. Rho, *Topological edge and corner states in a two-dimensional photonic Su-Schrieffer-Heeger lattice*, Nanophotonics **9**, 3227 (2020).

[57] C. H. Lee and R. Thomale, *Anatomy of skin modes and topology in non-Hermitian systems*, Physical Review B **99**, 201103 (2019).

[58] F. K. Kunst and V. Dwivedi, *Non-Hermitian systems and topology: A transfer-matrix perspective*, Physical Review B **99**, 245116 (2019).

[59] K. Kawabata, K. Shiozaki, M. Ueda, and M. Sato, *Symmetry and topology in non-Hermitian physics*, Physical Review X **9**, 041015 (2019).

[60] E. J. Bergholtz, J. C. Budich, and F. K. Kunst, *Exceptional topology of non-Hermitian systems*, Reviews of Modern Physics **93**, 015005 (2021).

[61] P. Delplace, D. Ullmo, and G. Montambaux, *Zak phase and the existence of edge states in graphene*, Physical Review B **84**, 195452 (2011).

[62] L. Ge and A. D. Stone, *Parity-time symmetry breaking beyond one dimension: The role of degeneracy*, Physical Review X **4**, 031011 (2014).

[63] H. Shackleton and M. S. Scheurer, *Protection of parity-time symmetry in topological many-body systems: Non-Hermitian toric code and fracton models*, Physical Review Research **2**, 033022 (2020).

[64] A. Yariv, Y. Xu, R. K. Lee, and A. Scherer, *Coupled-resonator optical waveguide: a proposal and analysis*, Opt. Lett. **24**, 711 (1999).

[65] M. J. Hartmann, F. G. S. L. Brandão, and M. B. Plenio, *Strongly interacting polaritons in coupled arrays of cavities*, Nature Physics **2**, 849 (2006).

[66] D. O. Krimer and R. Khomeriki, *Realization of discrete quantum billiards in a two-dimensional optical lattice*, Physical Review A **84**, 041807 (2011).

[67] G. Corrielli, A. Crespi, G. Della Valle, S. Longhi, and R. Osellame, *Fractional Bloch oscillations in photonic lattices*, Nature Communications **4**, 1555 (2013).

[68] F. Klauck, M. Heinrich, and A. Szameit, *Photonic two-particle quantum walks in Su–Schrieffer–Heeger lattices*, Photon. Res. **9**, A1 (2021).

[69] D. Jaksch, C. Bruder, J. I. Cirac, C. W. Gardiner, and P. Zoller, *Cold bosonic atoms in optical lattices*, Physical Review Letters **81**, 3108 (1998).

[70] I. Bloch, J. Dalibard, and W. Zwerger, *Many-body physics with ultracold gases*, Reviews of Modern Physics **80**, 885 (2008).

[71] G. Engelhardt, M. Benito, G. Platero, and T. Brandes, *Topologically enforced bifurcations in superconducting circuits*, Physical Review Letters **118**, 197702 (2017).

[72] Z. Yan, Y.-R. Zhang, M. Gong, Y. Wu, Y. Zheng, S. Li, C. Wang, F. Liang, J. Lin, Y. Xu *et al.*, *Strongly correlated quantum walks with a 12-qubit superconducting processor*, Science **364**, 753 (2019).

[73] M. Gong, S. Wang, C. Zha, M.-C. Chen, H.-L. Huang, Y. Wu, Q. Zhu, Y. Zhao, S. Li, S. Guo *et al.*, *Quantum walks on a programmable two-dimensional 62-qubit superconducting processor*, Science **372**, 948 (2021).

[74] D. Cheng, B. Peng, D.-W. Wang, X. Chen, L. Yuan, and S. Fan, *Arbitrary synthetic dimensions via multiboson dynamics on a one-dimensional lattice*, Physical Review Research **3**, 033069 (2021).

[75] A. Celi, P. Massignan, J. Ruseckas, N. Goldman, I. B. Spielman, G. Juzeliūnas, and M. Lewenstein, *Synthetic gauge fields in synthetic dimensions*, Physical Review Letters **112**, 043001 (2014).

[76] L. Yuan, Q. Lin, M. Xiao, and S. Fan, *Synthetic dimension in photonics*, Optica **5**, 1396 (2018).

[77] A. Dutt, Q. Lin, L. Yuan, M. Minkov, M. Xiao, and S. Fan, *A single photonic cavity with two independent physical synthetic dimensions*, Science **367**, 59 (2020).

[78] D. Yu, B. Peng, X. Chen, X.-J. Liu, and L. Yuan, *Topological holographic quench dynamics in a synthetic frequency dimension*, Light: Science & Applications **10**, 209 (2021).

[79] R. El-Ganainy, K. G. Makris, M. Khajavikhan, Z. H. Musslimani, S. Rotter, and D. N. Christodoulides, *Non-Hermitian physics and PT symmetry*, Nature Physics **14**, 11 (2018).

[80] M.-A. Miri and A. Alù, *Exceptional points in optics and photonics*, Science **363**, eaar7709 (2019).